[Chem. Pharm. Bull. 32(8)3164—3172(1984)]

Correlations between *in Vivo* and *in Vitro* Dissolution Rates of (α-Bromoisovaleryl)urea Polymorphs[1)]

HIROSHI KIWADA,* HIROYUKI KOJIMA, and YURIKO KATO

Faculty of Pharmaceutical Sciences, Science University of Tokyo, 12, Ichigaya Funagawara-machi, Shinjuku-ku, Tokyo 162, Japan

(Received September 28, 1983)

Correlations between the *in vivo* and *in vitro* dissolution rates of (α-bromoisovaleryl)urea polymorphs were investigated. The calculated dissolution rate constants obtained in the *in vitro* dissolution experiments were 0.135 and 0.133 (cm/min) for form I and form II, respectively. On the other hand, the crystals were administered intraduodenally into rats and the time course data of the plasma concentration were analyzed by the least-squares method on the basis of the Hixson–Crowell dissolution model for the intestinal dissolution process. The *in vivo* dissolution rate constants were obtained as 0.0629 and 0.0758 (cm/min) for form I and form II, respectively.

These *in vivo* and *in vitro* dissolution rate constants are based on the Noyes–Nernst dissolution theory and should be comparable in nature. Nevertheless, the *in vivo* rate constants were about a half of those *in vitro*. This result suggests that the stirring efficiency in the intestine is about a half of that of the *in vitro* dissolution experiment in this study.

Keywords——(α-bromoisovaleryl)urea; polymorph; pharmacokinetics; dissolution rate; dissolution rate constant; least-squares analysis; intestine; Noyes–Nernst model; Hixson–Crowell model

It is well known that the dissolution rate of crystals affects the absorption of drugs in the intestine. However, it has been considered difficult to relate the dissolution properties obtained in *in vitro* experiments to the *in vivo* pharmacokinetics, because the dissolution rate of crystals in the intestine is affected by the biological conditions, *e.g.* emptying time, secretions, or vermiculation of the intestine. Recently, Watari *et al.* studied the effect of particle size of sulfadimethoxine on the oral bioavailability, and demonstrated a relationship between the dissolution rates obtained from the blood concentrations by the deconvolution method and those predicted by the Hixson–Crowell model on the basis of *in vitro* dissolution experiments.[2)] More recently, Tanigawara *et al.* presented a method for evaluating the dissolution rate from the blood concentration data by the use of statistical moment theory.[3)]

We have investigated the bioavailability and dissolution properties of the polymorphic forms of (α-bromoisovaleryl)urea.[4,5)] In the previous report,[6)] a pharmacokinetic study on the fate of the drug was presented, with a kinetic model having a single first-order rate process for the dissolution-absorption process. However, these studies did not deal with the quantitative relationship of the *in vitro* dissolution rates of the crystals to the time courses of blood concentration after the oral administration of crystalline drugs.

In this study, the dissolution rate constants of the polymorphic forms of (α-bromoisovaleryl)urea obtained in *in vitro* dissolution experiments were applied to an intestinal dissolution model, and the time course data of the plasma concentrations after intraduodenal administration of the polymorphs were analyzed by a least-squares curve-fitting method. The correlations of the *in vivo* and *in vitro* dissolution rate constants are discussed.

Experimental

Preparation and Identification of (α-Bromoisovaleryl)urea Polymorphs——(α-Bromoisovaleryl)urea polymorphs

(form I and form II) were prepared and identified as described previously.[7]

Dissolution Experiments——Powdered (α-bromoisovaleryl)urea (about 2 g, 100—170 mesh) was suspended in 10 ml of 5% gelatin solution, and immediately added to 190 ml of water stirred with a Teflon plate (3.5 × 6 cm) at 150 rpm in a double-walled beaker at 37 °C. The samples were treated and determined as described previously.[4]

Animal Experiments——Wistar male rats, 180—220 g body weight, were fasted for one night before the experiment. The animals were cannulated with polyethylene tubing in the duodenal lumen and the femoral artery under ether anesthesia. Four mg (per 200 g body weight) of the powdered drug was suspended in 0.25 ml of 5% gelatin solution and administered into the duodenum, as described previously.[6] Blood samples were collected and the plasma concentrations of the drug were determined as in the previous study.[5]

Computations——Computations were carried out on the same computers and with the same programs for least-squares analyses as described in the previous paper.[6] Other programs for the model analyses and simulations presented here were written by the authors in Fortran.

Theoretical

The dissolution rate of a drug can generally be described by the Noyes–Nernst equation, which is based on the assumption that the dissolution process is rate-limited by diffusion from the thin layer of saturated solution at the solid surface into the bulk solution, as shown in Fig. 1.[8,9] The equation is as follows:

$$\frac{dC}{dt}=\frac{D\cdot S}{h\cdot V}\cdot(C_s-C)=k\cdot\frac{S}{V}\cdot(C_s-C)=K_n\cdot(C_s-C) \tag{1}$$

where D is the diffusion coefficient, h is the thickness of the diffusion layer, S is the surface area of the solid, V is the volume of dissolution medium, C_s is the saturated concentration, C is the concentration in the bulk solution, k ($=D/h$) is the dissolution rate constant which is used for the discussion in this paper, and K_n is the apparent dissolution rate constant in the Noyes–Nernst model.

The dissolved drug is immediately absorbed, because the absorption rate constant of (α-bromoisovaleryl)urea after intraduodenal administration of the solution is very large, as shown in the previous report ($K_a=0.712\,min^{-1}$).[6] Therefore, it is considered that the dissolution of the drug in the intestine meets the sink condition ($C\ll C_s$), and the particle size decreases in the process of absorption. The Noyes–Nernst equation can be transformed on the basis of the two assumptions described above in the following way[10] to describe the dissolution of an individual particle in the sink condition;

$$\frac{dW_i}{dt}=k\cdot S_i\cdot C_s=-k\cdot\pi\cdot a_i^2\cdot C_s \tag{2}$$

where W_i is the weight of the particle at time t, S_i ($=\pi\cdot a_i^2$) is the surface area of the particle, and a_i is the diameter of the particle. The weight of the particle is expressed as follows;

$$W_i=\frac{\pi\cdot a_i^3\cdot\rho}{6} \tag{3}$$

where ρ is the density of the particle. Differentiation of Eq. 3 with respect to time (t) gives,

$$\frac{dW_i}{dt}=\frac{\pi\cdot a_i^2\cdot\rho}{2}\cdot\frac{da_i}{dt} \tag{4}$$

By substituting Eq. 4 into Eq. 2 and rearranging the resultant equation, the following equation is obtained.

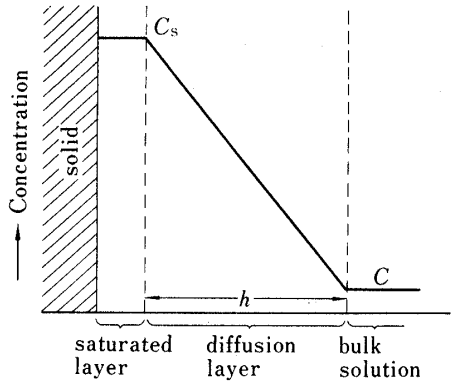

Fig. 1. Schematic Illustration of the Noyes–Nernst Dissolution Model

C_s; Saturated concentration.
C; Concentration in the bulk solution.
h; Thickness of diffusion layer.

$$da_i = \frac{-2 \cdot k \cdot C_s}{\rho} \cdot dt \tag{5}$$

By integrating Eq. 5 from time 0 to time t, the diameter of the particle is obtained as a function of time (t) as follows;

$$a_i = a_i^0 - \frac{2 \cdot k \cdot C_s}{\rho} \cdot t \tag{6}$$

where a_i^0 is the diameter of the particle at time 0. The cube root of W_i can be expressed as follows after the substitution of Eq. 6 into Eq. 3.

$$(W_i)^{1/3} = \left(\frac{\pi \cdot \rho}{6}\right)^{1/3} \cdot a_i = \left(\frac{\pi \cdot \rho}{6}\right)^{1/3} \cdot \left(a_i^0 - \frac{2 \cdot k \cdot C_s}{\rho} \cdot t\right) \tag{7}$$

The cube root of Eq. 3 at time 0 is as follows;

$$(W_i^0)^{1/3} = \left(\frac{\pi \cdot \rho}{6}\right)^{1/3} \cdot a_i^0 \tag{8}$$

After substituting Eq. 8 into Eq. 7, the following equation is obtained.

$$\sqrt[3]{W_i^0} - \sqrt[3]{W_i} = \left(\frac{\pi \cdot \rho}{6}\right)^{1/3} \cdot \frac{2 \cdot k \cdot C_s}{\rho} \cdot t \tag{9}$$

Assuming that the crystals are in the monodisperse state, the total weight of particles is expressed as follows;

$$W = N \cdot W_i \tag{10}$$

where N is the number of particles. After substituting Eq. 10 into Eq. 9, the Hixson–Crowell cube root equation is obtained.[11]

$$\sqrt[3]{W_0} - \sqrt[3]{W} = \left(\frac{\pi \cdot N \cdot \rho}{6}\right)^{1/3} \cdot \frac{2 \cdot k \cdot C_s}{\rho} \cdot t = \frac{2 \cdot k \cdot C_s \cdot \sqrt[3]{W_0}}{\rho \cdot a_0} \cdot t \tag{11}$$

where a_0 is the mean diameter of the particles at time 0, W_0 is the total weight of the drug at time 0, and W is the total weight of the undissolved drug at time t. The derivation of this equation is based on the assumption that the shape factors for cubic (or spherical) particles are constant as long as they dissolved equally from all sides.

The following differential equation derived from Eq. 11 is used for the pharmacokinetic model analysis,

$$\frac{dW}{dt} = -3 \cdot \frac{2 \cdot k \cdot C_s \cdot \sqrt[3]{W_0}}{\rho \cdot a_0} \cdot W^{2/3} = -K_d \cdot W^{2/3} \tag{12}$$

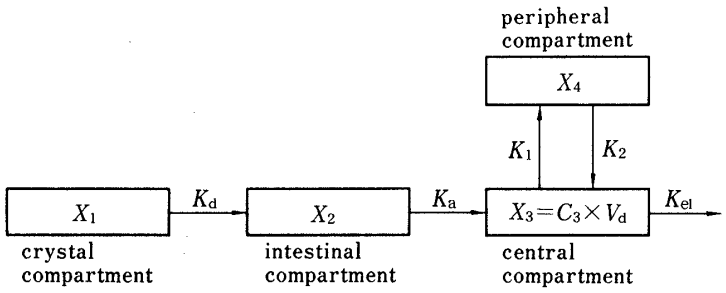

Fig. 2. Pharmacokinetic Model for *in Vivo* Behavior of (α-Bromoisovaleryl)urea after the Intraduodenal Administration of Crystals

X_1; Amount of crystalline drug in intestine.
X_2; Amount of dissolved drug in intestine.
X_3; Amount of drug in central compartment.
X_4; Amount of drug in peripheral compartment.
C_3; Concentration of drug in plasma.
V_d; Distribution volume.
K_d; Apparent dissolution rate constant in the Hixson–Crowell model.
K_a; First-order rate constant for absorption.
K_{el}; First-order rate constant for elimination.
K_1, K_2; First-order rate constant for transfer.

where K_d is the apparent dissolution rate constant in the Hixson–Crowell model.

Based on this model of the dissolution process in the intestine, the pharmacokinetic model shown in Fig. 2 is presented for the analysis of the *in vivo* data in relation to the dissolution properties of the crystals *in vitro*. The rate of change in the amount of the drug in each compartment of the model is described by the following differential equations.

$$\begin{aligned}
\frac{dX_1}{dt} &= -K_d \cdot X_1^{2/3} && [(1-F)\cdot X_0] \\
\frac{dX_2}{dt} &= K_d \cdot X_1^{2/3} - K_a \cdot X_2 && [F \cdot X_0] \\
\frac{dX_3}{dt} &= K_a \cdot X_2 - (K_1 + K_{e1}) \cdot X_3 + K_2 \cdot X_4 && [0] \\
\frac{dX_4}{dt} &= K_1 \cdot X_3 - K_2 \cdot X_4 && [0]
\end{aligned} \tag{13}$$

where X_0 is the weight administered, and F is the ratio of the dissolved drug in the gelatin solution to the dose at time 0, assessed from the *in vitro* experiments. Other expressions are shown in Fig. 2. Integrating under the initial conditions, as shown in the brackets following the equations at time 0, we obtain the plasma concentration of the drug as follows;

$$C_3 = A \cdot e^{-K_a \cdot t} + B \cdot e^{-p \cdot t} + C \cdot e^{-q \cdot t} + D \cdot t^2 + E \cdot t + FF \tag{14}$$

(see Appendix I)

However, Eq. 14 holds only while the crystals are present in the intestine. After the crystals are completely dissolved the following differential equations are obtained from the model shown in Fig.2 without the crystal compartment.

$$\begin{aligned}
\frac{dX_2}{dt} &= -K_a \cdot X_2 && [X_{02}] \\
\frac{dX_3}{dt} &= K_a \cdot X_2 - (K_1 + K_{e1}) \cdot X_3 + K_2 \cdot X_4 && [X_{03}] \\
\frac{dX_4}{dt} &= K_1 \cdot X_3 - K_2 \cdot X_4 && [X_{04}]
\end{aligned} \tag{15}$$

The disappearance time of crystals (T_0) was obtained by calculation from the apparent dissolution rate constant (K_d) found by curve fitting analysis based on the model shown in Fig. 2. The mean T_0 values of form I and form II were 62.6 and 34.9 min, respectively. Integrating Eq. 15 under the initial conditions described in the brackets following the equations, which are the calculated amounts of the drug in the compartments at time T_0 obtained by simulation, we obtained the time function of the plasma concentration after T_0 as follows;

$$C_3 = A \cdot e^{-K_a \cdot t} + B \cdot e^{-p \cdot t} + C \cdot e^{-q \cdot t} \tag{16}$$

(see Appendix II)

In order to compare the dissolution parameters obtained in the *in vitro* and *in vivo* experiments, the following derivations were carried out.

Integrating the Noyes–Nernst equation (Eq. 1) under the condition of constant surface area, we obtain the following equation.

$$\ln\left(\frac{C_s}{C_s - C}\right) = \frac{k \cdot S}{V} \cdot t = K_n \cdot t \tag{17}$$

The *in vitro* dissolution rate constant ($k_{in\ vitro}$) is calculated from the apparent dissolution rate constant (K_n) obtained in the *in vitro* dissolution experiment (Eq. 17) as follows;

$$k_{in\ vitro} = \frac{V}{S} \cdot K_n \tag{18}$$

On the other hand, the *in vivo* dissolution rate constant ($k_{in\ vivo}$) is calculated on Eq. 12 from the *in vivo* apparent dissolution rate constant (K_d) as follows;

$$k_{in\ vivo} = \frac{\rho \cdot a_0 \cdot K_d}{6 \cdot C_s \cdot \sqrt[3]{W_0}} \tag{19}$$

These two calculated dissolution rate constants ($k_{in\,vitro}$ and $k_{in\,vivo}$) should be comparable in nature because both rate constants are derived from the Noyes–Nernst dissolution theory (Eq. 1).

The derivations in this theory are based on the assumption of constant solubility with decreasing particle size in the intestinal compartment. On the other hand, it is known that the solubility of fine particles depends on the particle size[14] as given in the Ostwald–Freundlich equation;

$$\frac{\boldsymbol{R}\cdot T}{M}\cdot \ln\frac{C_s^2}{C_s^1}=\frac{2\cdot\gamma}{\rho}\cdot\left(\frac{1}{r_2}-\frac{1}{r_1}\right) \tag{20}$$

where C_s^1 and C_s^2 are the solubilities of particles with radii of r_1 and r_2, respectively, $\boldsymbol{R}$ is the gas constant, T is absolute temperature, M is molecular weight, ρ is density and γ is surface tension. In this experiment, the powdered drug was administered in gelatin solution. Therefore, the surface tension is reduced and it is assumed that the contribution of the particle size to the solubility in the intestine is negligible.

Results and Discussion

To obtain the dissolution parameters *in vitro*, plots based on Eq. 17 were drawn, as shown in Fig. 3. Linear plots were obtained. The apparent dissolution rate constants (K_n) were obtained from the slopes as 0.447 and 0.457 (min^{-1}) for form I and form II, respectively. The saturated concentration values were obtained from the previous dissolution experiments in gelatin solution[4] as 2.30 and 3.41 (mg/ml) for form I and form II, respectively. The condition of constant surface area assumed in the derivation of Eq. 17 should hold, since a large excess of crystals over that required for saturation was used, and the data were collected at the very early stage of the dissolution process, as shown in Fig. 3.

The *in vitro* dissolution rate constants ($k_{in\,vitro}$) were calculated by means of Eq. 18 as 0.135 and 0.133 (cm/min) for form I and form II, respectively. In this experiment, assuming that the powder is in the monodisperse particle state, the logarithmic mean diameter ($a_0 = 111.6\,\mu m$) was used for the mean diameter of the particles.[10] The density values of (α-bromoisovaleryl)urea polymorphs are given in the literature[12] as 1.62 g/cm^3 for form I and 1.56 g/cm^3 for form II. Form these values, the surface area of the particles was calculated based on Eq. 3 as follows;

$$S=\frac{6\cdot W_0}{\rho\cdot a_0} \tag{21}$$

The surface area of form I was 663.8 cm^2 and that of form II was 689.3 cm^2.

The intercepts of the straight lines shown in Fig. 3 suggest that a part of the drug had been dissolved before time 0 during the brief mixing of the crystals in the gelatin solution before the dissolution experiment.

The plasma concentration data after the intraduodenal administration of the polymorphs of (α-bromoisovaleryl)urea are shown in Fig. 4. The continuous lines in the figure are

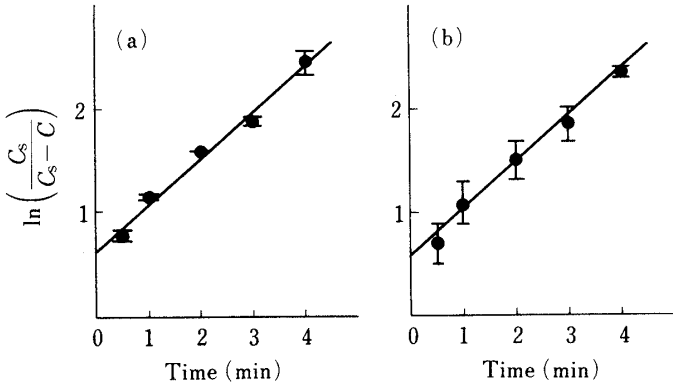

Fig. 3. Plots for Obtaining the Apparent Dissolution Rate Constant in the Noyes–Nernst Model

(a), form I; (b), form II. Points are each the mean ± S.E. of three experiments. Straight lines are those obtained by least-squares fitting.

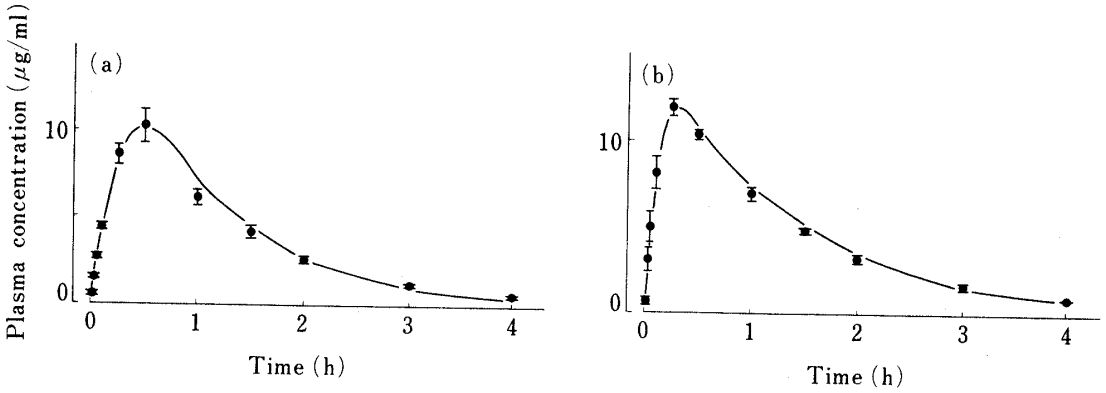

Fig. 4. Plasma Concentration after Intraduodenal Administration of (α-Bromoisovaleryl)urea Polymorphs

(a), form I; (b), form II. Points are each the mean ± S.E. of four rats. Continuous lines are those computed by the SALS program for the model shown in Fig. 2.

TABLE I. Pharmacokinetic Parameters Obtained by the Least-Squares Method Based on the Model Shown in Fig. 2

	K_d ($\mu g^{1/3} \cdot min^{-1}$)	K_a (min^{-1}) $\times 10^{-1}$	K_1 (min^{-1}) $\times 10^{-2}$	K_2 (min^{-1}) $\times 10^{-1}$	K_{el} (min^{-1}) $\times 10^{-2}$	V_d (ml)	F (%)
Form I	0.770±0.094	6.978±0.022	4.153±0.024	1.745±0.013	2.633±0.060	179.7±6.4	4.71±1.22
Form II	1.414±0.303	6.973±0.054	4.184±0.028	1.722±0.011	2.594±0.057	184.2±6.1	12.48±4.95

TABLE II. Dissolution Parameters Obtained in *in Vivo* and *in Vitro* Experiments

	Apparent dissolution rate constant		Intrinsic dissolution rate constant		$\frac{k_{invivo}}{k_{invitro}}$
	K_d ($\mu g^{1/3} \cdot min^{-1}$)	K_n (min^{-1})	k_{invivo} (cm/min)	$k_{invitro}$ (cm/min)	
Form I	0.770±0.094	0.447±0.015	0.0629±0.0077	0.135±0.004	0.47
Form II	1.414±0.262	0.457±0.033	0.0758±0.0141	0.133±0.010	0.57
Mean			0.0694±0.0013	0.134±0.008	0.52

calculated curves using the parameter values obtained by the least-squares curve-fitting analyses with the SALS program[13] based on the model shown in Fig. 2 before and after T_0 (time of consumption of crystals in the intestine) as described above. For the initial values of the parameters for the least-squares curve fitting, the values obtained in the previous experiment[6] were used except in the case of K_d. The calculated value from the k value obtained in the *in vitro* experiment described above was used as the initial value of K_d.

It seems reasonable to assume the validity of the pharmacokinetic model based on the Hixson–Crowell model in the intestine compartment, because the calculated curves showed better agreement with the experimental data (Fig. 4) than the first-order absorption model presented in the previous study.[6]

The parameter values obtained by the least-squares method are shown in Table I. The apparent dissolution rate constant (K_d) of form II was twice that of form I. The fraction of dissolved drug at the time of administration (F), caused by the mixing with the gelatin solution as suggested by the *in vitro* experiments mentioned above, of form II was 2.5 times

that of form I. Other kinetic parameter values were very similar for form I and form II. In the present model, the sink condition of the dissolution process in the intestine was confirmed by simulation of the concentration of the drug in the intestinal compartment, which showed that the maximum concentration was about 5—6% of the saturated concentration.

The parameter values obtained or calculated in the *in vivo* and *in vitro* experiments are listed in Table II. The apparent dissolution rate constants obtained in the *in vivo* experiment (K_d) showed significant differences ($p<0.05$) between form I and form II, as mentioned above, but in the *in vitro* experiment, there was no significant difference between form I and form II. However, these two apparent dissolution rate constants are different in nature, and thus are not strictly comparable.

On the other hand, the dissolution rate constants (k) calculated from the apparent rate constants are essentially the same in nature as mentioned previously. The calculated dissolution rate constants either *in vivo* or *in vitro* did not show significant differences between form I and form II. However, there were significant differences ($p<0.05$) between *in vivo* and *in vitro* values, and the dissolution rate constants *in vitro* are twice those *in vivo*, as shown in Table II.

In this study, it is demonstrated that the *in vitro* dissolution model can be introduced into the *in vivo* pharmacokinetics. However, the *in vivo* dissolution rate constants were about a half of those *in vitro*, and thus the dissolution process in the intestine was not fully reflected in the *in vitro* dissolution behavior. It is considered that this discrepancy is mainly caused by the stirring conditions, because, the calculated dissolution rate constant depends on the diffusion coefficient and the thickness of the saturated solution layer ($k=D/h$) as mentioned previously, and the former depends on the temperature and viscosity of medium, while the latter depends on the stirring efficiency. It is considered that there are only very small differences of viscosity and temperature between the *in vivo* and *in vitro* experiments, because both experiments were carried out at the same temperature (37 °C) in gelatin solution of same concentration. Therefore, it is concluded that the stirring efficiency of the intestine of rat is about a half of that in the *in vitro* dissolution experiment in this study.

This observation suggests that it is possible to introduce the dissolution parameters obtained in *in vitro* experiments into an *in vivo* study with the stirring factor of 0.5, and this has important implications for pharmacokinetic studies of the dissolution and absorption of crystalline drugs.

Appendix I

The time function of the plasma concentration in the model shown in Fig. 2 is as follows:

$$C_3=A\cdot e^{-K_a\cdot t}+B\cdot e^{-p\cdot t}+C\cdot e^{-q\cdot t}+D\cdot t^2+E\cdot t+FF$$

where

$$A=A_a+A_b;\qquad B=B_a+B_b;\qquad C=C_a+C_b$$

$$A_a=\frac{K_a\cdot(K_2-K_a)\cdot K_d\cdot\left[X_a^{2/3}\cdot K_a^2+\frac{2}{3}K_d\cdot X_a^{1/3}\cdot K_a+\frac{2}{9}K_d^2\right]}{-K_a^3\cdot(p-K_a)\cdot(q-K_a)\cdot V_d}$$

$$A_b=\frac{X_b\cdot K_a\cdot(K_2-K_a)}{V_d\cdot(p-K_a)\cdot(q-K_a)}$$

$$B_a=\frac{K_a\cdot(K_2-q)\cdot K_d\cdot\left[X_a^{2/3}\cdot p^2+\frac{2}{3}K_d\cdot X_a^{1/3}\cdot p+\frac{2}{9}K_d^2\right]}{-p^3\cdot(K_a-p)\cdot(q-p)\cdot V_d}$$

$$B_b=\frac{X_b\cdot K_a\cdot(K_2-p)}{V_d\cdot(K_a-p)\cdot(q-p)}$$

$$C_a=\frac{K_a\cdot(K_2-q)\cdot K_d\cdot\left[X_a^{2/3}\cdot q^2+\frac{2}{3}K_d\cdot X_a^{1/3}\cdot q+\frac{2}{9}K_d^2\right]}{-q^3\cdot(K_a-q)\cdot(p-q)\cdot V_d}$$

$$C_b=\frac{X_b\cdot K_a\cdot(K_2-q)}{V_d\cdot(K_a-q)\cdot(p-q)}$$

$$D=\frac{\frac{2}{9}K_d\cdot K_2}{2p\cdot q\cdot V_d}$$

$$E=\frac{\frac{2}{9}K_a\cdot K_d^3-\frac{2}{3}K_a\cdot K_2\cdot X_a^{1/3}-\frac{1}{2}D\cdot V_d\cdot(K_a\cdot p+q\cdot p+K_a\cdot q)}{V_d\cdot K_a\cdot p\cdot q}$$

$$FF=\frac{-\frac{2}{3}K_a\cdot K_d^2\cdot X_a^{1/3}+K_a\cdot K_2\cdot K_d\cdot X_a^{2/3}-\frac{1}{2}D\cdot V_d\cdot(K_a+p+q)-E\cdot V_d\cdot(K_a\cdot p+K_a\cdot q+p\cdot q)}{V_d\cdot K_a\cdot p\cdot q}$$

$$X_a=(1.0-F)\cdot X_0\,;\qquad X_b=F\cdot X_0$$

$$p=\frac{1}{2}[K_1+K_2+K_{e1})+\sqrt{(K_1+K_2+K_{e1})^2-4K_2\cdot K_{e1}}]$$

$$q=\frac{1}{2}[(K_1+K_2+K_{e1})-\sqrt{(K_1+K_2+K_{e1})^2-4K_2\cdot K_{e1}}]$$

Appendix II

The time function of the plasma concentration after the time (T_0) at which crystals are completely consumed by absorption is as follows:

$$C_3=A\cdot e^{-K_a\cdot t}+B\cdot e^{-p\cdot t}+C\cdot e^{-q\cdot t}$$

where

$$A=\frac{K_a\cdot(K_2-K_a)\cdot X_{02}}{V_d\cdot(p-K_a)\cdot(q-K_a)}$$

$$B=\frac{K_a\cdot(K_2-p)\cdot X_{02}+(K_a-p)\cdot(K_2-p)\cdot X_{03}+K_2\cdot(K_a-p)\cdot X_{04}}{V_d\cdot(K_a-p)\cdot(q-p)}$$

$$C=\frac{K_a\cdot(K_2-q)\cdot X_{02}+(K_a-q)\cdot(K_2-q)\cdot X_{03}+K_2\cdot(K_a-q)\cdot X_{04}}{V_d\cdot(K_a-q)\cdot(p-q)}$$

References and Notes

1) A part of this work was presented at the 102nd Annual Meeting of the Pharmaceutical Society of Japan, Osaka, April 1982.
2) N. Watari, M. Hanano, and N. Kaneniwa, *Chem. Pharm. Bull.*, **28**, 2221 (1980).
3) Y. Tanigawara, K. Yamaoka, T. Nakagawa, and T. Uno, Abstracts of Papers, the 102nd Annual Meeting of the Pharmaceutical Society of Japan, Osaka, April 1982, p. 609.
4) H. Kojima, H. Kiwada, and Y. Kato, *Chem. Pharm. Bull.*, **30**, 1824 (1982).
5) H. Kojima, H. Niimura, H. Kiwada, and Y. Kato, *Chem. Pharm. Bull.*, **30**, 1831 (1982).

6) H. Kiwada, H. Kojima, and Y. Kato, *Chem. Pharm. Bull.*, **31**, 1345 (1983).
7) H. Kiwada, K. Takami, and Y. Kato, *Chem. Pharm. Bull.*, **28**, 1351 (1980).
8) A. A. Noyes and W. R. Whitney, *J. Am. Chem. Soc.*, **19**, 930 (1897).
9) K. Sekiguchi, "Seizai Sekkei Hou (2)," ed. by K. Tsuda and H. Nogami, Chijin Shokan Pub. Ltd., Tokyo, 1974, pp. 94–114.
10) L. Z. Benet, "Dissolution Technology," ed. by L. T. Leeson and J. T. Carstensen, Acad. Pharm. Sci., Washington D.C., 1974, pp. 31–57.
11) A. W. Hixson and J. H. Crowell, *Ind. Eng. Chem.*, **23**, 923 (1931).
12) A. Watanabe, *Yakugaku Zasshi*, **58**, 565 (1928).
13) T. Nakagawa and Y. Oyanagi, "Recent Developments in Statistical Inference and Data Analysis," ed. by K. Matushita, North Holland Pub. Co., 1980, pp. 221–225.
14) T. Nadai and Y. Morimoto, "Pharmaceutics," ed. by T. Arita and H. Sezaki, Kodansha Scientific, Tokyo, 1980, pp. 84–129.